GROUP EXPECTATION POLICY OPTIMIZATION FOR STABLE HETEROGENEOUS REINFORCEMENT LEARNING IN LLMS

Han Zhang[1], **Ruibin Zheng**[2,1], **Zexuan Yi**[1], **Hanyang Peng**[1], **Hui Wang**[1], **Yue Yu**[1*]
[1] Peng Cheng Laboratory
[2] Guangzhou University

ABSTRACT

As the scale of single-center computing nodes approaches physical limits constrained by power capacity, decentralized distributed training is emerging as the predominant paradigm for future development. Reinforcement Learning (RL)-driven post-training, a critical pathway for enhancing the reasoning capabilities of Large Language Models (LLMs), typically alternates between homologous sampling (Rollout) and learning tasks in isomorphic environments. This approach struggles to adapt to the emerging demand for large-scale, decentralized training leveraging geographically distributed, asynchronous heterogeneous computing resources. To address this, we propose **HeteroRL**, an asynchronous RL architecture specifically designed for heterogeneous environments to efficient LLM mathematical reasoning training. HeteroRL decouples the Rollout sampler from the parameter learner, enabling deployment across distinct computing nodes and tolerating temporal delays induced by network transmission. We identify that high network latency impacts the RL training process primarily through increased KL divergence between the sampler and learner, ultimately causing importance sampling to fail due to excessive variance. However, internet network latency is inherently unpredictable. To mitigate this, we propose **Group Expectation Policy Optimization (GEPO)**, which reduces the variance of importance weights by refining the standard importance sampling calculation, thereby maintaining training stability and enhancing performance. Theoretically, we demonstrate that this method can exponentially reduce the variance of importance weights. Experiments on RL training with heterogeneous computing resources show that GEPO achieves superior training stability compared to popular methods like GRPO on mathematical reasoning benchmarks. Under extreme network delays of up to 1800 seconds, the performance degradation remains within 3% compared to single-center (synchronous) training, validating its significant potential for efficient decentralized distributed RL training in heterogeneous computing networks.

Keywords: Decentralized Training, Reinforcement Learning, Heterogeneous Computing, Large Language Models, Mathematical Reasoning, Importance Sampling

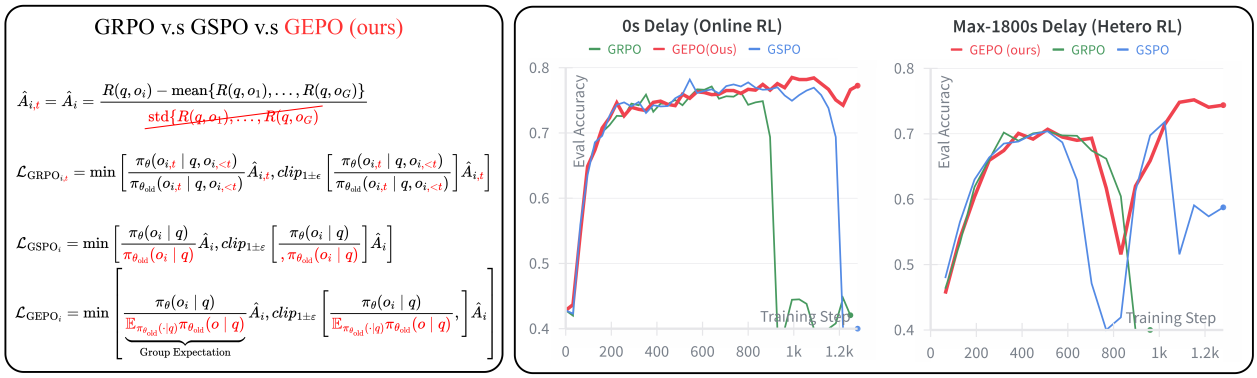

Figure 1: Left: GEPO improves upon GRPO and GSPO by employing sample-level importance sampling weights and group expectation smoothing to enhance training stability. Right: In both zero-delay (online) and high-delay (up to 1800 seconds) heterogeneous reinforcement learning scenarios, GEPO demonstrates superior stability and better evaluation performance (MATH-500).

* Corresponding author.

1 INTRODUCTION

In recent years, Large-scale Language Models (LLMs) (Dubey et al., 2024; Yang et al., 2025; Brown et al., 2020) have achieved remarkable progress through pre-training on massive text corpora. However, as high-quality pre-training data becomes increasingly scarce, the paradigm of solely relying on scaling up model size and data volume is encountering diminishing returns (Kaplan et al., 2020), with limited room for further performance improvement. To further unlock the potential of LLMs, particularly in enhancing their capabilities on complex tasks such as mathematical reasoning Shao et al. (2024), Reinforcement Learning (RL) (Bai et al., 2022; Jaques et al., 2020; Zhou & Xu, 2020; Kreutzer et al., 2018; Stiennon et al., 2020) has been widely adopted as an effective post-training method. RL allows the model to generate reasoning processes (e.g., chain-of-thought (Kojima et al., 2022)) through interaction with an environment and optimize based on reward signals (Shao et al., 2024) (e.g., the correctness of answers), thereby iteratively improving its reasoning abilities.

Despite the significant potential of RL in enhancing LLM reasoning, its large-scale distributed training faces serious systemic challenges. On the one hand, traditional synchronous RL frameworks require strict alternation between rollout generation and policy/critic updates (Han et al., 2025; Ji et al., 2023; Gao et al., 2023; Warnell et al., 2018). This leads to significant idle time for computational resources (e.g., GPUs) while waiting for the completion of the longest sequences when processing long reasoning outputs, severely constraining training efficiency (Fu et al., 2025). On the other hand, with the explosive growth in model size and data requirements, the computational power of a single node is no longer sufficient. Leveraging geographically distributed heterogeneous computing resources to form computing networks for decentralized training has become an inevitable trend (Team et al., 2025). In this scenario, network latency[1] between different nodes is inevitable, resulting in a temporal gap (i.e., delay or staleness) between the policy version used by the sampler and the latest policy version on the learner. Most existing RL frameworks are tightly coupled with homogeneous, low-latency computing environments and struggle to effectively address the challenges posed by such heterogeneity and latency, limiting their practical application in large-scale distributed deployments.

To address the above challenges, we propose HeteroRL (Heterogeneous Reinforcement Learning), a reinforcement learning framework specifically designed for asynchronous and heterogeneous environments, aiming to achieve efficient and robust mathematical reasoning training for large language models. The core idea of HeteroRL is to decouple the two computationally intensive yet distinct tasks in the RL pipeline—rollout sampling and parameter learning—and deploy them on independent computing nodes that may have different computational capabilities. The sampler is responsible for continuously generating reasoning trajectories, while the learner asynchronously updates the model parameters based on the collected trajectory data. Both processes run continuously without waiting for each other, communicating via dedicated networks or the internet to transfer model parameters and sampled data at low frequencies or under high latency. The heterogeneous reinforcement learning scenario differs from the traditional online reinforcement learning scenario, as shown in Table 1:

To address the challenge of policy version mismatch caused by network latency in heterogeneous distributed environments, we conduct an in-depth investigation and propose a novel reinforcement learning algorithm tailored for such settings. By designing a carefully crafted objective function, our method effectively balances training efficiency, convergence, and final model performance under dynamically varying communication delays.

Our findings reveal a particularly noteworthy insight: moderate temporal asynchrony does not necessarily harm model training—in fact, within a certain range, it can even improve both reasoning accuracy and training stability. **However, network latency is inherently constrained by real-world connectivity and is subject to high uncertainty in internet-based heterogeneous compute clusters. Our experiments demonstrate that excessive delay has a catastrophic effect on importance sampling, significantly inflating the variance of importance weights and thereby degrading both training stability and the achievable performance ceiling.**

In summary, our key contributions are as follows:

Framework Design: We propose HeteroRL, an asynchronous reinforcement learning framework designed for heterogeneous compute networks, enabling decentralized deployment for mathematical reasoning training in large language models (LLMs).

Key Insight: We identify a strong correlation between network latency and the KL divergence between the rollout sampler and the learner. Excessive KL divergence induced by high latency leads to training instability and eventual collapse.

Algorithmic Innovation: We introduce Group Expectation Policy Optimization (GEPO), which improves upon the importance sampling mechanism in GRPO (Shao et al., 2024). We provide theoretical justification that GEPO substan-

[1] In this paper, the terms 'delay' and 'latency' are used interchangeably.

Table 1: Core Characteristics of Online, Offline, and Heterogeneous Reinforcement Learning Paradigms

Aspect	Online RL	Offline RL	Heterogeneous RL
Data Generation	Online interaction: Data generated instantly by the **current policy**.	Fixed, pre-collected dataset: Uses **static data** collected by some (unknown) behavior policy.	Delayed interaction: Data generated by **historical policy versions** (due to **unpredictable network delay**).
Policy Version during Data Generation	**Always current**: Requires strict synchronization with the learning policy.	**Fixed**: The behavior policy is fixed and inherent to the dataset.	**Dynamically stale**: Staleness determined by **unpredictable network delay** *(core characteristic)*.
System Architecture	Tightly-coupled: **Actor (environment interaction)** and **Learner (parameter update)** typically co-located or on a low-latency network.	Single-machine or simple distributed: **No real-time interaction** required; training is data-driven.	Geographically decoupled: **Actor and Learner separated** by a **high-latency network**, tolerant to delays.
Handling of System Latency	Treated as failure: Requires synchronization; latency causes **resource idling** and training stalls.	Not applicable: Training process has **no real-time interaction**.	**Algorithmic compensation**: Employs **corrective techniques** (e.g., importance sampling) to mitigate latency effects.
Core Challenge	**Exploration-exploitation** trade-off during learning. *Resource utilization* under sequential tasks.	**Distributional shift** and **limited data coverage**.	**Algorithmic stability under dynamic delays**: High/variable latency causes **importance weight variance explosion***.

Note: *High variance in importance weights is a critical challenge identified in Heterogeneous RL due to dynamic delays.

tially reduces the variance of importance weights under large policy divergence, and empirically show that it enhances both stability and efficiency of RL training under high network latency.

Experimental Validation: Extensive experiments on mathematical reasoning benchmarks demonstrate that HeteroRL achieves superior performance and stability compared to existing synchronous baselines.

This work not only offers new system and algorithmic perspectives for overcoming data bottlenecks in pretraining and unlocking the post-training potential of LLMs, but also lays a practical foundation for building large-scale distributed AI training systems adapted to future heterogeneous compute network infrastructures.

2 BACKGROUND

2.1 PROBLEM DEFINITION AND NOTATION

Consider a standard policy gradient framework. Let π_θ denote the language model policy (i.e., the Actor) parameterized by θ, x be an input prompt (e.g., a math problem), and $y = (y_1, \ldots, y_T)$ be the output sequence generated by the model (e.g., a chain-of-thought solution). The environment provides a scalar reward $r(y)$ based on the outcome of y (e.g., whether the final answer is correct). We define the following core notation:

- π_{θ_k} (short for q): the policy used by the *sampler* at time step k to generate rollout trajectories.
- $\pi_{\theta_{k+\tau}}$ (short for p): the latest policy at the *learner* at time step $k + \tau$, used for gradient updates.
- τ: *policy staleness*, representing the discrepancy in policy versions between the sampler and the learner, caused by network transmission delays and computational asynchrony. In our setting, τ is a random variable rather than a fixed constant.
- y: a trajectory sampled from the stale policy π_{θ_k}.
- $r(x, y)$: the reward for response y given input x.

- $A(x, y)$: the advantage for response y to input x, typically defined as $A(x, y) = r(x, y) - b(x)$, where $b(x)$ is a baseline reward computed for input x.

The goal of RL is to optimize the policy π_θ to maximize the expected cumulative reward:

$$\max_\theta \mathbb{E}_{y\sim\pi_\theta(\cdot|x)}[r(y)]. \tag{1}$$

Since this objective is not directly differentiable with respect to θ, the policy gradient theorem is typically applied, leading to the optimization of the following equivalent, differentiable surrogate objective:

$$\mathcal{L}(\theta) = \mathbb{E}_{y\sim\pi_\theta(\cdot|x)}\left[r(y)\sum_{t=1}^{T}\nabla_\theta \log \pi_\theta(y_t|x)\right]. \tag{2}$$

In practice, to reduce the variance of the gradient estimator, an advantage function $A(y)$ is introduced. The advantage function measures how much better the reward $r(y)$ of a generated trajectory y is compared to a baseline. A common choice for the baseline is the average reward over multiple sampled trajectories for the same input. Thus, the objective is rewritten as:

$$\mathcal{L}(\theta) = \mathbb{E}_{y\sim\pi_\theta(\cdot|x)}\left[A(y)\sum_{t=1}^{T}\nabla_\theta \log \pi_\theta(y_t|x)\right]. \tag{3}$$

In this paper, we adopt the within-group average reward as used in GRPO (Shao et al., 2024):

$$b(x) = \frac{1}{G}\sum_{j=1}^{G} r(x, y_j). \tag{4}$$

2.2 GRPO: Group Relative Policy Optimization

Group Relative Policy Optimization (GRPO) is an efficient reinforcement learning algorithm designed specifically for post-training of large language models (LLMs). The key idea of GRPO is to eliminate the complex critic network used in PPO, and instead compute the advantage function using relative rewards among multiple sampled responses to the same input. Specifically, for each input question x, the model generates a group of G candidate responses, and the advantage $A(x, y_i)$ is normalized using the mean reward of the group as a baseline:

$$A(y_i) = r(y_i) - \frac{1}{G}\sum_{j} r(x, y_j). \tag{5}$$

This approach not only significantly reduces computational overhead but also provides more stable optimization through within-group relative comparison. The GRPO objective resembles that of PPO, combining a clipped importance sampling term with a direct KL regularization term to prevent excessive policy deviation. However, like PPO, GRPO still uses token-level importance ratios:

$$w_{i,t}(\theta) = \frac{p(y_{i,t}|x, y_{i,<t})}{q(y_{i,t}|x, y_{i,<t})}. \tag{6}$$

GRPO applies clipping and gradient computation at each token. This token-level optimization can introduce high-variance gradient noise in long sequences or Mixture-of-Experts (MoE) models, leading to training instability or even irreversible model collapse (Zheng et al., 2025). Moreover, since the importance weights operate at the token level rather than the full sequence level, there is a mismatch with the sequence-level reward signal, which theoretically undermines the effectiveness of importance sampling. To address these issues, the Qwen Team (Zheng et al., 2025) proposed Group Sequence Policy Optimization (GSPO), which defines the importance ratio at the sequence level as:

$$s_i(\theta) = \left(\frac{p(y_i|x)}{q(y_i|x)}\right)^{\frac{1}{|y_i|}}. \tag{7}$$

It performs unified clipping and optimization over the entire response sequence. This better aligns the reward unit with the optimization unit, significantly improving training stability and efficiency, especially for RL training of large-scale MoE models.

2.3 Core Challenge: Off-Policy Learning and Importance Sampling

This formulation highlights the central challenge in asynchronous RL: the mismatch between the behavior policy (π_{θ_k}) and the target policy ($\pi_{\theta_{k+\tau}}$), which grows with τ and introduces bias and variance into the learning process. Addressing this mismatch under high and uncertain latency is the primary focus of our work.

The HeteroRL framework decouples rollout sampling from parameter learning, leading to a setting where the learner updates the new policy $\pi_{\theta_{k+\tau}}$ using data generated by an older policy π_{θ_k}—a canonical off-policy learning scenario. To correct for the distributional shift between the behavior and target policies, importance sampling (IS) is commonly employed. Under the GRPO framework, this weight is used to scale the advantage during policy gradient updates. However, when the delay τ is large, causing significant divergence between the policies (i.e., high KL divergence $D_{\mathrm{KL}}(\pi_{\theta_{k+\tau}} \| \pi_{\theta_k})$), we observe in practice that the variance of the importance weights increases rapidly with τ, and the estimation error of the expected reward also grows. As a result, the variance of w_{std} explodes, introducing high noise into gradient estimates and ultimately leading to training instability or collapse. The central challenge of this work is thus to design a robust algorithm that mitigates the training instability caused by the explosion of importance sampling variance under high network latency.

2.4 Overview of HeteroRL

The overview of HeteroRL is illustrated in Figure 2. By decoupling sampling and training, HeteroRL enables decentralized distributed RL training of LLMs across five compute nodes: one parameter update node (learner) and four data generation nodes (sampler), forming a star-shaped network topology. Network delays between the sampler and learner nodes are explicitly modeled and can be simulated using stochastic distributions such as the log-normal or Weibull distribution.

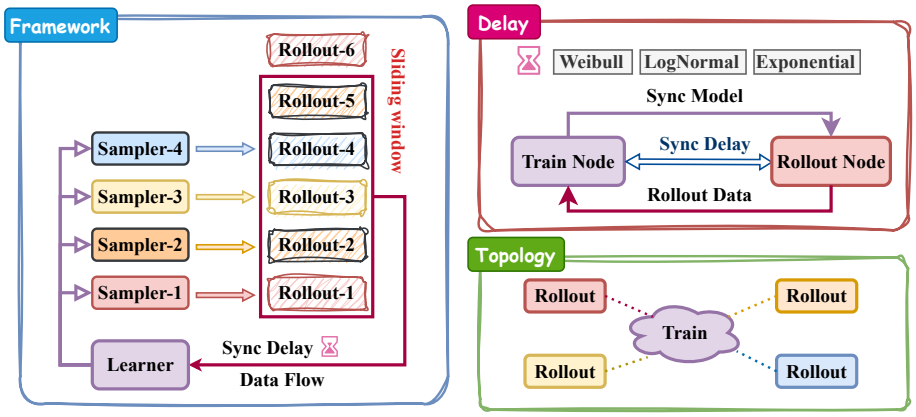

Figure 2: The Overview of HeteroRL.

3 GEPO: Group Expectation Policy Optimization

Our method builds upon the group-based policy optimization paradigm of GRPO and introduces the **Group Expectation Smoothing** (GES) mechanism. We emphasize a paradigm shift from *token-level* to *sample-level* importance weighting, which significantly reduces the variance of importance weights and alleviates gradient instability during training.

3.1 From Token-Level to Sample-Level Importance Weighting

In traditional policy optimization methods, importance sampling is typically performed at the *token level*. Specifically, for a generated sequence $y = (y_1, \ldots, y_T)$, the importance weight is computed token by token:

$$w_t = \mathrm{clip}\left(\frac{p(y_t \mid x, y_{<t})}{q(y_t \mid x, y_{<t})}, 1-\epsilon, 1+\epsilon\right), \tag{8}$$

and used to compute the policy gradient at each time step. However, this per-token reweighting scheme suffers from two key limitations:

1) Inconsistency between optimization and reward granularity: Concurrent work such as GSPO argues that since the reward is assigned at the sequence level—i.e., to the full response y—the importance weighting for policy updates should also operate at the same granularity, rather than at the token level.

2) High variance in token-level probabilities: Beyond this alignment issue, we provide an explanation from the perspective of importance weight variance: because the final reward depends on the entire sample, large local changes in token probabilities can lead to extreme values in the ratio $\frac{p(y_t|x,y_{<t})}{q(y_t|x,y_{<t})}$. This inflates the variance of token-level importance weights, causing them to frequently fall outside the clipping range. Once clipped, gradients for these tokens are effectively zeroed out due to the stop-gradient behavior of `torch.clamp`, preventing meaningful updates. As a result, tokens that require large corrections may be ignored, leading to inefficient optimization.

To address these issues, we adopt *sample-level* importance weighting: treating the entire response y as a single sampling unit and computing the weight based on its full conditional probability. Given a prompt x, both the target policy $p(y|x)$ and the behavior policy $q(y|x)$ are defined as the joint probability of the sequence:

$$p(y|x) = \left| \prod_{t=1}^{T} p(y_t \mid x, y_{<t}) \right|^{\frac{1}{T}}, \quad q(y|x) = \left| \prod_{t=1}^{T} q(y_t \mid x, y_{<t}) \right|^{\frac{1}{T}}. \tag{9}$$

The standard sample-level importance weight is then:

$$w_{\text{std}}(y|x) = \text{clip}\left(\frac{p(y|x)}{q(y|x)}, 1-\epsilon, 1+\epsilon \right). \tag{10}$$

This formulation computes the full sequence-level ratio before clipping, thereby avoiding premature truncation caused by high-variance individual tokens. By preserving gradient flow across the entire sequence, sample-level weighting enables more stable and effective policy updates, especially under high policy divergence induced by network latency.

3.2 Group Expectation Importance Weighting

To enhance the stability of importance weights, we propose the *Group Expectation Importance Weight* (GEIW) mechanism, which replaces the individual proposal probability $q(y|x)$ in the standard importance weight $\frac{p(y|x)}{q(y|x)}$ with its group-wise expected value under the current prompt x, denoted as $\widehat{\mathbb{E}}_q[q(y|x)]$. Inspired by GRPO, for each input x, we generate a group of K responses $\{y_1, \ldots, y_K\} \sim q(\cdot|x)$ to form a sampling group. Since K is typically much smaller than the full policy space and top-P/top-K sampling leads to $\sum_{i=1}^{K} q(y_i|x) \gg 1$, the vector $(q(y_1|x), \ldots, q(y_K|x))$ does not constitute a valid probability distribution. Simply using the arithmetic mean $\frac{1}{K}\sum_{i=1}^{K} q(y_i|x)$ would introduce bias due to ignoring the relative sampling probabilities. To obtain a more accurate estimate, we employ a weighted expectation:

$$\widehat{\mathbb{E}}_q[q(y|x)] = \sum_{i=1}^{K} q(y_i|x) \cdot \widehat{q(y_i|x)} = \frac{\sum_{i=1}^{K} q(y_i|x)^2}{\sum_{i=1}^{K} q(y_i|x)}, \tag{11}$$

where $\widehat{q(y_i|x)} = \frac{q(y_i|x)}{\sum_{j=1}^{K} q(y_j|x)}$ is the within-group normalized probability, serving as an empirical estimate of the sampling likelihood of each y_i. We define the GEIW importance weight as:

$$w_{\text{GEIW}}(y|x) = \frac{p(y|x)}{\widehat{\mathbb{E}}_q[q(y|x)]}. \tag{12}$$

The key advantages of this mechanism are as follows:

- **Stability**: The denominator is decoupled from any single $q(y|x)$, avoiding extreme weight values when individual proposal probabilities approach zero.
- **Robustness**: By leveraging within-group statistical information, GEW provides a more reliable scale estimate. Even under large divergence between p and q, $\widehat{\mathbb{E}}_q[q(y|x)]$ remains well-conditioned, effectively preventing gradient explosion. Although this estimator introduces a small bias, both theoretical analysis (see Theorem 1) and empirical results demonstrate that it significantly reduces variance under high KL divergence, yielding more stable gradient directions and improved training convergence.

Theorem 1. *Let p, q be discrete probability distributions. Then there exists a constant C such that:*

$$\text{Var}\left[\frac{p(y|x)}{q(y|x)} \right] - \text{Var}\left[\frac{p(y|x)}{\widehat{\mathbb{E}}_q[q(y|x)]} \right] \geq \exp\left(D_{\text{KL}}(p\|q) \right) - C. \tag{13}$$

In particular, when $D_{\mathrm{KL}}(p\|q) > \log C$, it holds that

$$\mathrm{Var}\left[\frac{p(y|x)}{q(y|x)}\right] > \mathrm{Var}\left[\frac{p(y|x)}{\widehat{\mathbb{E}}_q[q(y|x)]}\right]. \tag{14}$$

Theorem 1 shows that GEPO can **exponentially reduce the variance of importance weights**, making it particularly well-suited for heterogeneous RL training under high KL divergence. The full mathematical proof is provided in Appendix A. However, the inequality equation 14 does not always hold. As shown in Figure 3, we visualize the relationship between KL divergence and importance weight variance when both p and q are Bernoulli or Gaussian distributions with varying parameters. The results indicate that in the high-KL regime, the group expectation approach significantly reduces the variance of importance weights, which benefits training stability under high network latency. Nevertheless, there exist regimes—such as the green regions in the plots—where our method incurs a slight increase in variance.

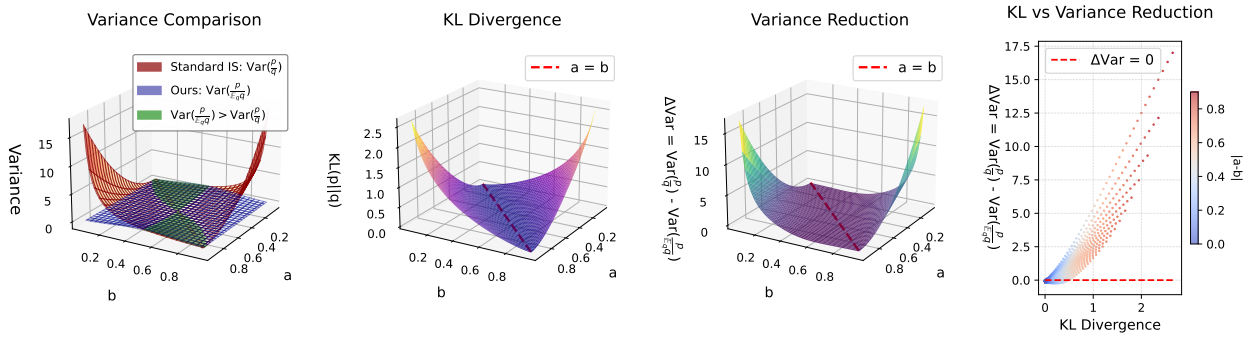

(a) Variance comparison of $\frac{p}{q}$ and $\frac{p}{\mathbb{E}_q[q]}$ under Bernoulli distributions, where $p \sim \text{Bernoulli}(a)$ and $q \sim \text{Bernoulli}(b)$.

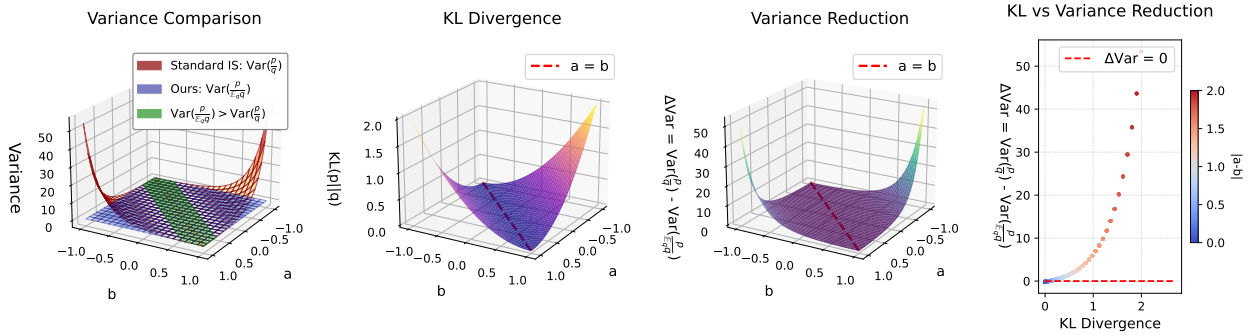

(b) Variance comparison of $\frac{p}{q}$ and $\frac{p}{\mathbb{E}_q[q]}$ under Gaussian distributions, where $p \sim \mathcal{N}(a, 1)$ and $q \sim \mathcal{N}(b, 1)$.

Figure 3: In high-KL regions, $\mathrm{Var}[\frac{p(y|x)}{\widehat{\mathbb{E}}_q[q(y|x)}] \ll \mathrm{Var}[\frac{p(y|x)}{q(y|x)}]$.

3.3 Defensive Sampling and Smooth Denominator Mechanism

To mitigate potential bias introduced by replacing the denominator and further enhance robustness, we introduce a defensive sampling mechanism that incorporates the target policy probability into the denominator:

$$w_{\text{final}}(y|x) = \frac{p(y|x)}{\epsilon \cdot p(y|x)\texttt{.detach()} + (1-\epsilon) \cdot \widehat{\mathbb{E}}_q[q(y|x)]}, \tag{15}$$

where $\epsilon \propto \mathrm{Var}(q) \in (0, 1)$ is a smoothing coefficient, and $p(y|x)\texttt{.detach()}$ denotes stopping gradient propagation during backpropagation. We employ a heuristic strategy that sets ϵ proportional to the variance of q, which we find in most experimental settings leads to improved training stability. A higher $\mathrm{Var}(q)$ indicates greater bias from using the GEIS approximation (i.e., larger $(q - \widehat{\mathbb{E}}_q[q(y|x)])^2$), so increasing ϵ reduces reliance on the potentially biased $\widehat{\mathbb{E}}_q[q(y|x)]$ and shifts the objective toward the policy gradient update.

Notably, the standard policy gradient objective $\log p(y|x) \cdot A(x, y)$ produces gradients of the form $\frac{p'_\theta(y|x) \cdot A(x,y)}{p(y|x).\texttt{detach()}}$, which is equivalent to the gradient induced by $w_{\text{final}}(y|x) \cdot A(x, y)$ when $\epsilon = 1$. Since policy gradients do not rely on importance sampling, they are inherently immune to high variance in importance weights under large network delays. This design exhibits the following properties:

- When $p(y|x)$ is high, the denominator adapts locally, preserving the weight magnitude for high-probability samples;
- When $\mathrm{Var}(q)$ is low, the denominator reverts to the group average, avoiding numerical instability;
- When $\mathrm{Var}(q)$ is high, the objective smoothly transitions toward the policy gradient update, avoiding the detrimental effects of high-variance importance weights;
- The overall weighting scheme produces smoother weight distributions and reduced gradient variance, leading to more stable and efficient training under asynchronous, heterogeneous conditions.

4 EXPERIMENTS

4.1 EXPERIMENTAL SETUP

Dataset and Benchmarks We conduct reinforcement learning training and evaluation on the Qwen3-1.7B model using the MATH lv.3–5 dataset, reporting average Pass@1 over 8 sampled responses. We compare our method against baseline methods GRPO and GSPO under both homogeneous and heterogeneous computing settings.

Heterogeneous Computing Environment We perform heterogeneous training across five compute nodes: one learner node and four sampler nodes, forming a star-shaped topology centered at the learner. During training, the sampler nodes generate rollout data, which is transmitted over the network to the learner node in a streaming fashion. The learner updates the model parameters and periodically broadcasts the updated weights back to the sampler nodes. The learner processes incoming rollouts in the order they arrive, operating within a fixed time window for data eligibility. Since data is transmitted in batch units—each containing text, generation probabilities, and rewards—a maximum delay of 1800 seconds is sufficient for typical network conditions. Within this window, the iteration gap (in terms of gradient updates) between the learner and samplers remains within 64 steps.

Simulated Network Delay Configuration Our goal is to simulate RL training of large models over internet-connected heterogeneous compute clusters, where network delays are inherently uncertain. To evaluate algorithmic performance and training stability under extreme and variable latency conditions, we employ three widely used delay distributions P_d: log-normal, Weibull, and exponential. We set a high maximum delay threshold of 1800 seconds, which is sufficient to cover typical model and data transmission times. In our simulation, model parameter synchronization and rollout data transfer are implemented as follows:

- **Learner saves model:** The learner periodically saves model checkpoints to a shared model file path `Model_Sync_Path` via `torch.save_pretrained()`.
- **Sampler loads model:** The sampler generates data using the current model until a delay D_M, drawn from P_d, elapses. It then loads the latest model from `Model_Sync_Path`. The sampler remains active throughout—no idling occurs.
- **Sampler sends data:** Generated rollout batches are saved to *Rollout_Sync_Path* with timestamp T_{sync}. To simplify implementation, data transmission is assumed instantaneous; its latency is effectively merged into the model sync delay D_M, without affecting simulation validity.
- **Learner uses data:** The learner trains on rollout data from `Rollout_Sync_Path` that falls within a recent time window (e.g., no older than 1800 seconds).

Implementation Details All experiments are conducted on the Qwen3-1.7B-Instruct model, using `bfloat16` precision and Flash Attention-2 to accelerate attention computation. The training framework follows a GRPO-like algorithm with a learning rate of 1×10^{-6}, employing a constant learning rate schedule with 3% linear warmup. The per-device batch size is set to 8, with a gradient accumulation step of 1. Gradient checkpointing is enabled to reduce memory consumption. Evaluation is performed every 32 or 64 training steps, depending on the configuration. To simulate network latency in heterogeneous computing environments, we introduce a log-normal distributed delay simulator. The simulated delay is bounded between 60 seconds (minimum) and 1800 seconds (maximum), with a 99.5% confidence interval. The default delay is set to 60 seconds. The maximum allowed policy staleness—measured in effective delayed

steps—is varied at 0, 4, 8, 16, 32, and 64 steps in different ablation settings. For the online scenario, we do not use KL divergence for optimization, for the heterogeneous scenario, we uniformly adopt CPPO-KL (Zhang et al., 2024) loss with a coefficient of 0.005. We employ vLLM for efficient rollout inference, with the GPU memory utilization cap set to 0.45 and 8 parallel responses generated per prompt to compute group-wise advantages. Each experiment runs for 3 training epochs, and all training metrics are logged via Weights & Biases (wandb). The system prompt used in the experiments is shown in Figure 4.

> You are a helpful AI Assistant, designed to provided well-reasoned and detailed responses. You FIRST think about the reasoning process as an internal monologue and then provide the user with the answer. Please put your final answer within \boxed{}. Also, indicate that it is the answer.

Figure 4: System prompt of all trainings in our experiments.

The only difference across all compared methods lies in the computation of the importance weights, as detailed in Listing 1:

```
if self.loss_type == "grpo":
    coef_1 = learner_token_p / sampler_token_p
elif self.loss_type == "gspo":
    coef_1 = learner_seq_p / sampler_seq_p
elif self.loss_type == "gepo":
    normalized_q = sampler_seq_p.detach() / (sampler_seq_p.sum().detach())
    coef_1 = learner_seq_p / (normalized_q * sampler_seq_p).sum()
```

Listing 1: Coefficient computation for different policy optimization methods

4.2 Real-World Network Scenarios

To evaluate the performance of heterogeneous reinforcement learning algorithms in realistic network environments, we develop a communication toolkit based on ZeroMQ, supporting TCP/IP-based transmission of inference trajectories from samplers to learners and synchronized model parameter updates. The toolkit enables multi-node communication over wide-area networks (WANs), with the following core communication logic:

- The learner continuously listens for and buffers inference trajectory messages from samplers. It automatically updates its trajectory buffer upon message arrival and broadcasts the latest model parameters to all connected samplers once a predefined synchronization interval is reached.
- After generating an inference trajectory, the sampler sends it to the learner and continuously listens for parameter update messages. Upon receiving a new model or reaching a local synchronization condition, the sampler updates its local parameters and resumes sampling.

Key features of the communication toolkit include:

1) Many-to-Many Communication Pattern The system supports elastic node scaling with dynamically reconfigurable routing topologies, enabling seamless adaptation to node join/leave events. This facilitates efficient distributed parameter synchronization and trajectory collection in large-scale deployments.

2) Chunked Message Transmission Inspired by Shardcast, the toolkit employs adaptive message chunking for both model parameters and trajectory data. The chunk size is dynamically adjusted according to real-time bandwidth conditions. At the receiver side, chunks are reassembled and integrity-verified, effectively mitigating the impact of high latency in wide-area networks.

3) Communication Safety Mechanisms Thread-safe message passing across multiple processes is ensured via a double-buffering queue design and fine-grained locking. This prevents race conditions during concurrent read/write operations and guarantees reliable parameter synchronization.

4) Configurable Routing Topology The toolkit supports user-defined connectivity patterns between learners and samplers, accommodating asymmetric node configurations (e.g., one learner connected to four samplers). This enhances communication efficiency and scalability in dynamic, heterogeneous environments.

4.3 Main Experimental Results

As shown in Table 2, for the Qwen3-1.7B backbone model, GEPO achieved the highest average performance among all policy optimization methods, demonstrating its effectiveness. It is worth noting that GRPO experienced a sharp performance drop in the third epoch of training. While GSPO could somewhat delay this performance collapse, it still could not avoid the eventual degradation. In contrast, GEPO perfectly suppressed the occurrence of such collapses, exhibiting only minor fluctuations.

Table 2: Performance of different policy optimization methods on the MATH500 mathematical dataset

Method	**Max Tolerable Delay 0**		**Max Tolerable Delay 8**		**Max Tolerable Delay 64**	
	Best	**Last**	**Best**	**Last**	**Best**	**Last**
GRPO	77.1	41.2	73.3	44.6	70.2	27.3
GSPO	78.2	31.6	74.5	60.4	71.8	58.7
GEPO (ours)	**78.5**	**77.3**	**75.8**	**75.7**	**75.3**	**74.4**

From the experimental results in Table 2, it can be observed that GEPO outperforms existing state-of-the-art methods in both optimal performance and final performance, regardless of whether in zero-delay or high-delay scenarios. During the training process of GRPO and GSPO, after reaching a performance peak, they are prone to training collapse, resulting in a significant gap between their final performance and best performance. Figure 5 records one set of training processes. From the training curves, it can be seen that GEPO is more stable compared to GRPO and GSPO, with consistently lower variance of importance weights and no significant changes in gradient norms, thus the reward value shows no obvious decline at the end of training. In this experiment, we used identical hyperparameters (such as a KL penalty of 0.005 to maintain training stability) and the same random seed to ensure rollout data consistency as much as possible. None of the methods employed defensive sampling mechanisms.

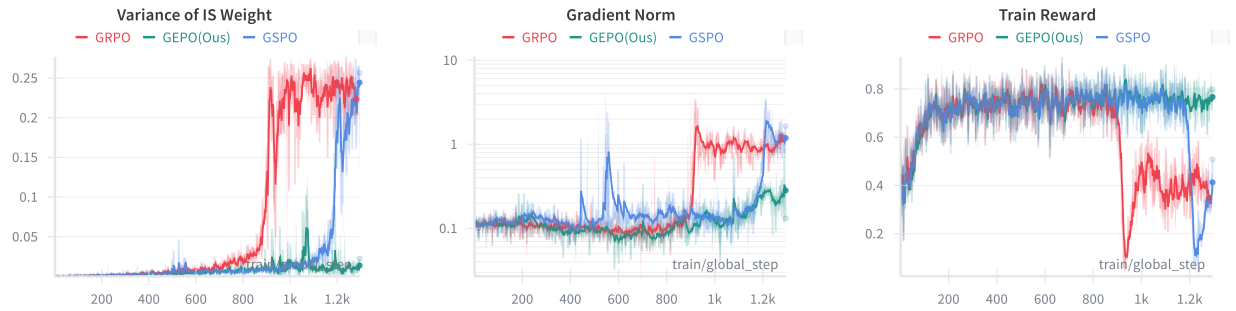

(a) Variance of importance weights increases at step 900

(b) Gradient norm becomes unstable starting at step 900

(c) Training reward begins to decline sharply at step 900

Figure 5: Synchronous changes in importance sampling variance, training gradient norm, and training reward. Compared to GRPO and GSPO, our proposed GEPO maintains more stable importance weight variance, resulting in less drastic gradient changes, more stable training, and no decline in training reward.

4.4 Analysis Studies

Impact of Latency As shown in Figure 6, we analyze the changes in KL divergence between the trainer and sampler, variance of importance weights, and estimation error of the expected value of the advantage function (optimization objective) during heterogeneous RL training as latency increases. We observe that latency leads to increased KL divergence (Figure 6a), which in turn causes an increase in the variance of importance weights (Figure 6b), ultimately resulting in increased estimation error of the expected advantage function (Figure 6c). Since the optimization objec-

tive is to maximize the estimated expectation of the advantage function, large estimation errors will cause significant fluctuations in gradients, thereby affecting training stability and performance.

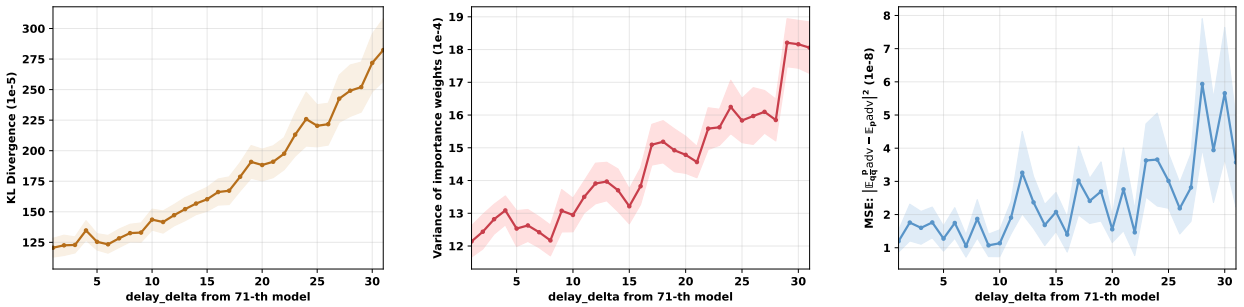

(a) KL-divergence increases with delay steps

(b) Variance of importance weights increases with delay steps

(c) Estimation error of $\mathbb{E}[adv(x, y)]$ vs. delay steps

Figure 6: Trends of latency and importance sampling variance

Correlation Analysis Figure 7 further analyzes the correlation between training delay steps, importance sampling variance, and estimation error of the expected advantage function. We find that the correlation coefficients among these three variables range from 0.76 to 0.96 ($\alpha = 0.05$), indicating that higher latency leads to greater training instability. However, we observe that changes in KL divergence are not solely related to latency but also depend on the model and sampled data. While higher latency increases the probability of KL divergence spikes, it does not always lead to training collapse.

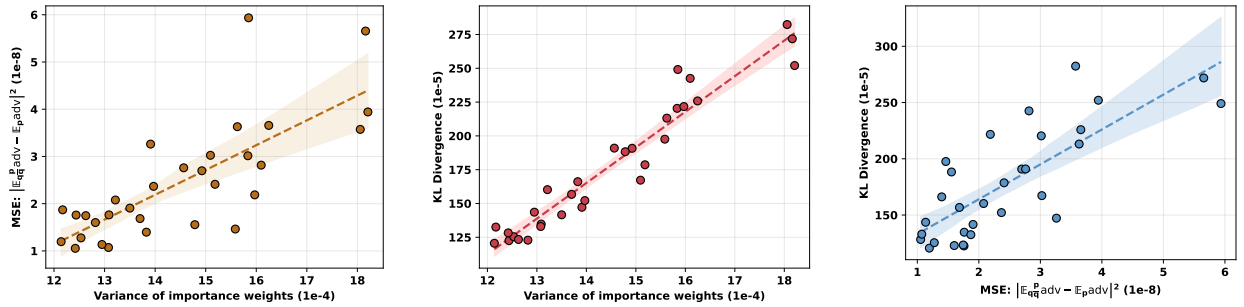

(a) The correlation between importance weight variance and estimation error of $\mathbb{E}_p[adv(x, y)]$ is **0.76**.

(b) The correlation between importance weight variance and KL divergence is **0.96**.

(c) The correlation between KL divergence and $\mathbb{E}_p[adv(x, y)]$ estimation error is **0.78**.

Figure 7: Correlation analysis (**95% CI**) of training delay steps, importance sampling variance, and estimation error of expected advantage function

Challenges of High Latency To demonstrate that high latency reduces training stability, we compared training processes with maximum delays of 8 steps and 64 steps respectively. As shown in Figure 8, under the maximum delay of 64 steps, particularly when the delay reaches its peak (around step 900), the KL divergence increases rapidly and the evaluation accuracy significantly decreases. This experiment confirms our hypothesis that latency increases instability. Although GEPO significantly improves training stability compared to methods like GRPO, it is still affected by latency-induced issues (performance drop around step 900), indicating that heterogeneous reinforcement learning in high-latency scenarios remains a challenging research direction. Better methods should be able to mitigate the negative impact of latency on training, making the training process more stable.

5 Related Work

In recent years, as reinforcement learning (RL) has become increasingly central to post-training of large language models (LLMs) Ziegler et al. (2019), researchers have begun to recognize the efficiency bottlenecks of traditional

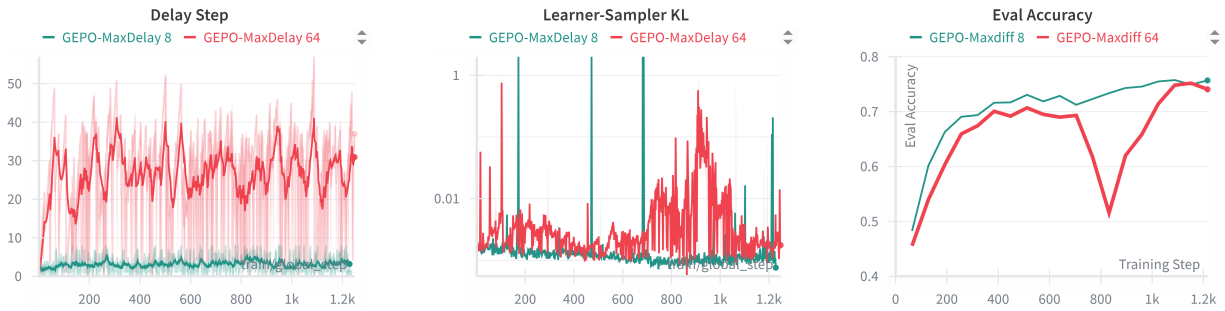

(a) Delay steps of the sampler (b) Variation of KL divergence (c) Evaluation accuracy curve

Figure 8: Training processes under different latency conditions

synchronous RL frameworks. Noukhovitch et al. (2024) were among the first to theoretically explore the feasibility of asynchronous RLHF(Ouyang et al., 2022), proposing a paradigm that decouples generation and learning phases to enable "on-policy yet off-policy" RLHF. Their work demonstrates that different RL algorithms exhibit varying degrees of robustness to off-policy data, with Online DPO Calandriello et al. (2024) showing exceptional resilience—even under high levels of policy mismatch. More importantly, they observe that larger policy models tend to be more robust to off-policy data, providing theoretical justification for asynchronous training in large-scale models. Wu. et;al introduces LlamaRL Wu et al. (2025), a fully distributed and asynchronous reinforcement learning framework designed to enhance the efficiency and scalability of large language model training by decoupling generation and optimization to reduce idle GPU time and improve resource utilization. This foundational work establishes the viability of asynchronous RLHF but primarily focuses on single-machine or small-scale cluster settings, leaving the challenges of dynamic network delays in heterogeneous environments largely unaddressed.

To tackle practical efficiency limitations, recent efforts have turned toward system-level implementations. AREAL Fu et al. (2025) proposes a fully asynchronous RL system that eliminates resource idling by completely decoupling the generation and training pipelines. The system introduces staleness thresholds for training and a decoupled PPO (Schulman et al., 2017) objective to effectively handle samples generated by outdated policy versions. Experiments on mathematical reasoning and code generation tasks show that AREAL not only significantly improves training efficiency—reducing end-to-end training time compared to synchronous systems—but also surprisingly enhances final model performance. However, AREAL is primarily designed for language reasoning tasks under relatively stable network conditions and does not adequately account for the dynamically varying delays inherent in geographically distributed, heterogeneous compute networks. This stands in contrast to the core challenge addressed by HeteroRL: how to maintain training stability and efficiency under unpredictable, high-latency network conditions. While AREAL provides valuable insights and a strong baseline, its limitations highlight the need for a more robust and delay-tolerant framework—motivating the design and contributions of our work. Prime Intellect Team et al. (2025) proposes a decentralized, asynchronous RL framework that enables scalable reasoning model training on community-owned compute by addressing trust issues through verifiable inference, ensuring training stability via two-sided GRPO clipping, and supporting controllable reasoning through length-aware rewards.

6 Conclusion

This paper proposes the HeteroRL framework and the GEPO algorithm, effectively addressing the stability challenges of reinforcement learning training for large language models in heterogeneous computing networks. By decoupling Rollout sampling from parameter learning, HeteroRL enables asynchronous training across geographically distributed heterogeneous nodes, adapting to high-latency network environments. To tackle the issues of exacerbated policy staleness and exploding importance sampling variance caused by high latency, we propose the GEPO algorithm, which employs sample-level importance weight calculation and introduces a Group Expectation Smoothing mechanism, significantly reducing the variance of gradient estimation. Theoretical analysis demonstrates that GEPO provides superior variance control compared to standard importance sampling when KL divergence is large. Experimental results validate the effectiveness of our approach on the MATH-500 mathematical reasoning task: even under extreme network latency conditions of up to 1800 seconds, GEPO maintains training stability, with model performance degradation limited to within 3% compared to synchronous training, significantly outperforming baseline methods such as GRPO and GSPO.

This research provides a viable pathway for building efficient and robust decentralized reinforcement learning systems for large models, advancing the evolution of AI training paradigms in heterogeneous computing environments.

AUTHOR CONTRIBUTIONS

The division of labor within the research team is as follows: **Han Zhang** was responsible for the design of the GEPO algorithm, preliminary implementation of the HeteroRL training framework, and technical report writing. **Ruibin Zheng** focused on optimizing the HeteroRL training framework code, improving data transmission execution logic in simulated latency scenarios, optimizing model hyperparameters and prompts, creating visualizations, and conducting model performance testing. **Zexuan Yi** was responsible for implementing data transmission in real network environments and engineering the model synchronization mechanism; the theoretical proofs in the article were verified by **Xiang Li**. The defensive sampling mechanism was initially proposed by the **Qwen3-235B-A22B-2507 model**. While our experiments demonstrated that this mechanism can enhance training stability, we note that no existing literature has formally documented or proposed such a defensive sampling mechanism.

ACKNOWLEDGMENTS

This work is supported by the Major Key Project of PCL (Grant No. PCL2025AS209).

REFERENCES

Yuntao Bai, Saurav Kadavath, Sandipan Kundu, Amanda Askell, Jackson Kernion, Andy Jones, Anna Chen, Anna Goldie, Azalia Mirhoseini, Cameron McKinnon, et al. Constitutional ai: Harmlessness from ai feedback. *ArXiv Preprint ArXiv:2212.08073*, 2022.

Tom Brown, Benjamin Mann, Nick Ryder, Melanie Subbiah, Jared D Kaplan, Prafulla Dhariwal, Arvind Neelakantan, Pranav Shyam, Girish Sastry, Amanda Askell, Sandhini Agarwal, Ariel Herbert-Voss, Gretchen Krueger, Tom Henighan, Rewon Child, Aditya Ramesh, Daniel Ziegler, Jeffrey Wu, Clemens Winter, Chris Hesse, Mark Chen, Eric Sigler, Mateusz Litwin, Scott Gray, Benjamin Chess, Jack Clark, Christopher Berner, Sam McCandlish, Alec Radford, Ilya Sutskever, and Dario Amodei. Language models are few-shot learners. In *Proceedings of the International Conference on Neural Information Processing Systems*, pp. 1877–1901, 2020.

Daniele Calandriello, Daniel Guo, Remi Munos, Mark Rowland, Yunhao Tang, Bernardo Avila Pires, Pierre Harvey Richemond, Charline Le Lan, Michal Valko, Tianqi Liu, et al. Human alignment of large language models through online preference optimisation. *arXiv preprint arXiv:2403.08635*, 2024.

Abhimanyu Dubey, Abhinav Jauhri, Abhinav Pandey, Abhishek Kadian, Ahmad Al-Dahle, Aiesha Letman, Akhil Mathur, Alan Schelten, Amy Yang, Angela Fan, et al. The llama 3 herd of models. *ArXiv Preprint ArXiv:2407.21783*, 2024.

Wei Fu, Jiaxuan Gao, Xujie Shen, Chen Zhu, Zhiyu Mei, Chuyi He, Shusheng Xu, Guo Wei, Jun Mei, Jiashu Wang, et al. Areal: A large-scale asynchronous reinforcement learning system for language reasoning. *arXiv preprint arXiv:2505.24298*, 2025.

Leo Gao, John Schulman, and Jacob Hilton. Scaling laws for reward model overoptimization. In *Proceedings of the 40th International Conference on Machine Learning*, pp. 10835–10866, 2023.

Zhenyu Han, Ansheng You, Haibo Wang, Kui Luo, Guang Yang, Wenqi Shi, Menglong Chen, Sicheng Zhang, Zeshun Lan, Chunshi Deng, et al. Asyncflow: An asynchronous streaming rl framework for efficient llm post-training. *arXiv preprint arXiv:2507.01663*, 2025.

Natasha Jaques, Judy Hanwen Shen, Asma Ghandeharioun, Craig Ferguson, Agata Lapedriza, Noah Jones, Shixiang Gu, and Rosalind Picard. Human-centric dialog training via offline reinforcement learning. In *Proceedings of the 2020 Conference on Empirical Methods in Natural Language Processing)*, pp. 3985–4003, 2020.

Jiaming Ji, Tianyi Qiu, Boyuan Chen, Borong Zhang, Hantao Lou, Kaile Wang, Yawen Duan, Zhonghao He, Jiayi Zhou, Zhaowei Zhang, et al. Ai alignment: A comprehensive survey. *ArXiv Preprint ArXiv:2310.19852*, 2023.

Jared Kaplan, Sam McCandlish, Tom Henighan, Tom B Brown, Benjamin Chess, Rewon Child, Scott Gray, Alec Radford, Jeffrey Wu, and Dario Amodei. Scaling laws for neural language models. *ArXiv Preprint ArXiv:2001.08361*, 2020.

Takeshi Kojima, Shixiang Shane Gu, Machel Reid, Yutaka Matsuo, and Yusuke Iwasawa. Large language models are zero-shot reasoners. *Advances in neural information processing systems*, 35:22199–22213, 2022.

Julia Kreutzer, Shahram Khadivi, Evgeny Matusov, and Stefan Riezler. Can neural machine translation be improved with user feedback? In *Proceedings of the 2018 Conference of the North American Chapter of the Association for Computational Linguistics*, pp. 92–105, 2018.

Michael Noukhovitch, Shengyi Huang, Sophie Xhonneux, Arian Hosseini, Rishabh Agarwal, and Aaron Courville. Asynchronous rlhf: Faster and more efficient off-policy rl for language models. *arXiv preprint arXiv:2410.18252*, 2024.

Long Ouyang, Jeffrey Wu, Xu Jiang, Diogo Almeida, Carroll Wainwright, Pamela Mishkin, Chong Zhang, Sandhini Agarwal, Katarina Slama, Alex Ray, et al. Training language models to follow instructions with human feedback. *Advances in neural information processing systems*, 35:27730–27744, 2022.

John Schulman, Filip Wolski, Prafulla Dhariwal, Alec Radford, and Oleg Klimov. Proximal policy optimization algorithms. *arXiv preprint arXiv:1707.06347*, 2017.

Zhihong Shao, Peiyi Wang, Qihao Zhu, Runxin Xu, Junxiao Song, Xiao Bi, Haowei Zhang, Mingchuan Zhang, YK Li, Yang Wu, et al. Deepseekmath: Pushing the limits of mathematical reasoning in open language models. *arXiv preprint arXiv:2402.03300*, 2024.

Nisan Stiennon, Long Ouyang, Jeff Wu, Daniel M. Ziegler, Ryan Lowe, Chelsea Voss, Alec Radford, Dario Amodei, and Paul Christiano. Learning to summarize from human feedback. In *Proceedings of the International Conference on Neural Information Processing Systems*, pp. 3008–3021, 2020.

Prime Intellect Team, Sami Jaghouar, Justus Mattern, Jack Min Ong, Jannik Straube, Manveer Basra, Aaron Pazdera, Kushal Thaman, Matthew Di Ferrante, Felix Gabriel, et al. Intellect-2: A reasoning model trained through globally decentralized reinforcement learning. *arXiv preprint arXiv:2505.07291*, 2025.

Garrett Warnell, Nicholas Waytowich, Vernon Lawhern, and Peter Stone. Deep tamer: Interactive agent shaping in high-dimensional state spaces. In *Proceedings of the AAAI conference on artificial intelligence*, pp. 1545–1553, 2018.

Bo Wu, Sid Wang, Yunhao Tang, Jia Ding, Eryk Helenowski, Liang Tan, Tengyu Xu, Tushar Gowda, Zhengxing Chen, Chen Zhu, et al. Llamarl: A distributed asynchronous reinforcement learning framework for efficient large-scale llm trainin. *arXiv preprint arXiv:2505.24034*, 2025.

An Yang, Anfeng Li, Baosong Yang, Beichen Zhang, Binyuan Hui, Bo Zheng, Bowen Yu, Chang Gao, Chengen Huang, Chenxu Lv, Chujie Zheng, Dayiheng Liu, Fan Zhou, Fei Huang, Feng Hu, Hao Ge, Haoran Wei, Huan Lin, Jialong Tang, Jian Yang, Jianhong Tu, Jianwei Zhang, Jianxin Yang, Jiaxi Yang, Jing Zhou, Jingren Zhou, Junyang Lin, Kai Dang, Keqin Bao, Kexin Yang, Le Yu, Lianghao Deng, Mei Li, Mingfeng Xue, Mingze Li, Pei Zhang, Peng Wang, Qin Zhu, Rui Men, Ruize Gao, Shixuan Liu, Shuang Luo, Tianhao Li, Tianyi Tang, Wenbiao Yin, Xingzhang Ren, Xinyu Wang, Xinyu Zhang, Xuancheng Ren, Yang Fan, Yang Su, Yichang Zhang, Yinger Zhang, Yu Wan, Yuqiong Liu, Zekun Wang, Zeyu Cui, Zhenru Zhang, Zhipeng Zhou, and Zihan Qiu. Qwen3 technical report. *arXiv preprint arXiv:2505.09388*, 2025.

Han Zhang, Yu Lei, Lin Gui, Min Yang, Yulan He, Hui Wang, and Ruifeng Xu. Cppo: Continual learning for reinforcement learning with human feedback. In *The Twelfth International Conference on Learning Representations*, 2024.

Chujie Zheng, Shixuan Liu, Mingze Li, Xiong-Hui Chen, Bowen Yu, Chang Gao, Kai Dang, Yuqiong Liu, Rui Men, An Yang, et al. Group sequence policy optimization. *arXiv preprint arXiv:2507.18071*, 2025.

Wangchunshu Zhou and Ke Xu. Learning to compare for better training and evaluation of open domain natural language generation models. *Proceedings of the AAAI Conference on Artificial Intelligence*, 34(05):9717–9724, 2020.

Daniel M Ziegler, Nisan Stiennon, Jeffrey Wu, Tom B Brown, Alec Radford, Dario Amodei, Paul Christiano, and Geoffrey Irving. Fine-tuning language models from human preferences. *arXiv preprint arXiv:1909.08593*, 2019.

A THEORETICAL PROOF OF IMPORTANCE SAMPLING VARIANCE

This appendix analyzes a newly proposed importance sampling weight $w_{\text{new}}(x) = \dfrac{p(x)}{\mathbb{E}_q[q]}$, where $\mathbb{E}_q[q] = \int q(x)^2 dx$, and compares its variance with the standard importance sampling weight $w_{\text{std}}(x) = \dfrac{p(x)}{q(x)}$.

Problem Setting Let the target distribution be $p(x)$ and the proposal distribution be $q(x)$. We aim to estimate:

$$\mathbb{E}_p[f] = \int f(x)p(x)dx. \tag{16}$$

Since direct sampling from p is difficult, we employ importance sampling by drawing samples from q.

Standard Importance Sampling The standard weight is defined as:

$$w_{\text{std}}(x) = \frac{p(x)}{q(x)}. \tag{17}$$

Its expectation under q is:

$$\mathbb{E}_q\left[\frac{p(x)}{q(x)}\right] = \int \frac{p(x)}{q(x)} q(x)dx = \int p(x)dx = 1, \tag{18}$$

thus it is unbiased. Its variance is:

$$\begin{aligned} \text{Var}_q(w_{\text{std}}) &= \mathbb{E}_q\left[\left(\frac{p}{q}\right)^2\right] - \left(\mathbb{E}_q\left[\frac{p}{q}\right]\right)^2 \\ &= \int \frac{p(x)^2}{q(x)}dx - 1. \end{aligned} \tag{19}$$

Denoted as:

$$\text{Var}_{\text{std}} = \int \frac{p(x)^2}{q(x)}dx - 1. \tag{20}$$

Group Expectation Importance Sampling The new weight is defined as:

$$w_{\text{new}}(x) = \frac{p(x)}{\mathbb{E}_q[q]}, \quad \text{where} \quad \mathbb{E}_q[q] = \int q(x)^2 dx. \tag{21}$$

Its expectation is:

$$\mathbb{E}_q[w_{\text{new}}] = \frac{1}{\mathbb{E}_q[q]} \int p(x)q(x)dx = \frac{\langle p, q\rangle}{\|q\|_2^2}, \tag{22}$$

where $\langle p, q\rangle$ denotes the inner product $\int p(x)q(x)dx$. Generally, $\langle p, q\rangle \neq \|q\|_2^2$, making this estimator biased. Its variance is:

$$\begin{aligned} \text{Var}_q(w_{\text{new}}) &= \mathbb{E}_q\left[\left(\frac{p(x)}{\mathbb{E}_q[q]}\right)^2\right] - \left(\mathbb{E}_q\left[\frac{p(x)}{\mathbb{E}_q[q]}\right]\right)^2 \\ &= \frac{1}{(\mathbb{E}_q[q])^2}\left(\int p(x)^2 q(x)dx - \left(\int p(x)q(x)dx\right)^2\right). \end{aligned} \tag{23}$$

Denoted as:

$$\text{Var}_{\text{new}} = \frac{1}{\left(\int q(x)^2 dx\right)^2}\left(\int p(x)^2 q(x)dx - \left(\int p(x)q(x)dx\right)^2\right). \tag{24}$$

Variance Comparison We compare:

$$\boxed{\begin{aligned} \text{Var}_{\text{std}} &= \int \frac{p(x)^2}{q(x)}dx - 1, \\ \text{Var}_{\text{new}} &= \frac{1}{\left(\int q(x)^2 dx\right)^2}\left(\int p(x)^2 q(x)dx - \left(\int p(x)q(x)dx\right)^2\right). \end{aligned}} \tag{25}$$

A.1 VARIANCE COMPARISON IN DISCRETE SPACE

Since the action space of large models is discrete, this section discusses the variance difference $\Delta = \mathrm{Var}_{\text{std}} - \mathrm{Var}_{\text{new}}$ in discrete probability space. The integral expressions in the continuous case naturally transition to discrete summation forms:

- Replace continuous integrals $\int \cdot dx$ with discrete summations $\sum_{i=1}^{n}$;
- Replace probability density functions $p(x)$, $q(x)$ with probability masses p_i, q_i;
- Maintain the structural form of variance expressions unchanged.

Notation and Setting Let the sample space be a finite set $\mathcal{X} = \{1, 2, \ldots, n\}$, where $n \geq 2$. Let $p = (p_1, \ldots, p_n)$ and $q = (q_1, \ldots, q_n)$ be two probability distributions satisfying:

- $p_i > 0, \sum_{i=1}^{n} p_i = 1$,
- $q_i > 0, \sum_{i=1}^{n} q_i = 1$.

Define the following four key quantities, corresponding to the integral terms in the continuous expressions:

$$A = \left(\sum_{i=1}^{n} q_i^2\right)^2, \qquad \text{(corresponding to } \left(\int q(x)^2 dx\right)^2\text{)} \tag{26}$$

$$B = \left(\sum_{i=1}^{n} p_i q_i\right)^2, \qquad \text{(corresponding to } \left(\int p(x)q(x)dx\right)^2\text{)} \tag{27}$$

$$I_1 = \sum_{i=1}^{n} \frac{p_i^2}{q_i}, \qquad \text{(corresponding to } \int \frac{p(x)^2}{q(x)}dx\text{)} \tag{28}$$

$$I_2 = \sum_{i=1}^{n} p_i^2 q_i, \qquad \text{(corresponding to } \int p(x)^2 q(x)dx\text{)} \tag{29}$$

Accordingly, the variance difference can be written as:

$$\Delta = I_1 + \frac{B - A - I_2}{A}. \tag{30}$$

Lemma 1 (Range of Quantities)**.** *Under the above setting, we have:*

- $A \in \left[\frac{1}{n^2},\ 1\right]$,
- $B \in [0,\ 1]$,
- $I_1 \in [1,\ \infty)$,
- $I_2 \in (0,\ 1]$.

Proof.
1. Range of A: By the power mean inequality, $\sum q_i^2 \geq \frac{1}{n}$, and $\sum q_i^2 \leq 1$, thus $A \in [1/n^2, 1]$.
2. Range of B: $\sum p_i q_i \in (0, 1]$, thus $B \in [0, 1]$.
3. Range of I_1: By the Cauchy-Schwarz inequality, $I_1 \geq 1$, and it can approach infinity.
4. Range of I_2: Since $p_i^2 \leq p_i$, we have $I_2 \leq 1$, and $I_2 > 0$. □

Theorem 1. Let p, q be discrete probability distributions. Then there exists a constant C such that:

$$\mathrm{Var}\left[\frac{p(y|x)}{q(y|x)}\right] - \mathrm{Var}\left[\frac{p(y|x)}{\widehat{\mathbb{E}}_q[q(y|x)]}\right] \geq \exp\left(D_{\mathrm{KL}}(p\|q)\right) - C. \tag{31}$$

In particular, when $D_{\mathrm{KL}}(p\|q) > \log C$, it holds that $\mathrm{Var}[\frac{p(y|x)}{q(y|x)}] > \mathrm{Var}[\frac{p(y|x)}{\widehat{\mathbb{E}}_q[q(y|x)]}]$.

Proof. **Step 1.** From the fundamental inequality relationship between KL divergence and χ^2 divergence (Pinsker's inequality):

$$D_{\mathrm{KL}}(p\|q) \leq \log\left(1 + D_{\chi^2}(p\|q)\right), \tag{32}$$

where the chi-square divergence is defined as:

$$D_{\chi^2}(p\|q) = \sum_{i=1}^{n} \frac{(p_i - q_i)^2}{q_i} = \sum_{i=1}^{n} \frac{p_i^2}{q_i} - 1 = I_1 - 1. \tag{33}$$

Substituting yields:

$$D_{\mathrm{KL}}(p\|q) \leq \log(I_1), \tag{34}$$

therefore:

$$I_1 \geq \exp\left(D_{\mathrm{KL}}(p\|q)\right). \tag{35}$$

Step 2. From Lemma 1, we know that A, B, and I_2 satisfy the following bounds:

$$A \in [\frac{1}{n^2}, 1], \tag{36}$$

$$B \in [0, 1], \tag{37}$$

$$I_2 \in (0, 1]. \tag{38}$$

Consider the lower bound of the expression $\dfrac{B - A - I_2}{A}$. To obtain its minimum value, we take:

- Minimum value of B: $B = 0$
- Minimum value of A: $A = \frac{1}{n^2}$
- Maximum value of I_2: $I_2 = 1$

Substituting yields:

$$\frac{B - A - I_2}{A} \geq \frac{0 - 1/n^2 - 1}{1/n^2} = -(n^2 + 1). \tag{39}$$

Step 3. Substituting inequalities (1) and (2) into the expression for Δ:

$$\Delta = I_1 + \frac{B - A - I_2}{A} \geq \exp\left(D_{\mathrm{KL}}(p\|q)\right) - (n^2 + 1). \tag{40}$$

When $D_{\mathrm{KL}}(p\|q) > \log(n^2 + 1)$, we have:

$$\exp\left(D_{\mathrm{KL}}(p\|q)\right) > n^2 + 1, \tag{41}$$

thus:

$$\Delta > 0, \tag{42}$$

i.e., $\mathrm{Var}_{\mathrm{std}} > \mathrm{Var}_{\mathrm{new}}$. □

Corollary 1. *In discrete space, if $D_{KL}(p\|q) > \log(n^2 + 1)$, then:*

$$\mathrm{Var}_{std} > \mathrm{Var}_{new}, \tag{43}$$

i.e., the new estimator has smaller variance.

It should be noted that A only attains the value $\frac{1}{n^2}$ when q follows a uniform distribution. In practice, when large models generate responses, the distribution tends to be long-tailed, so the value of A is closer to 1, and the constant $C \ll \log(n^2 + 1)$.